ChemComm

Accepted Manuscript

This article can be cited before page numbers have been issued, to do this please use: X. Ma, X. Shi, S. Bai, J. Zhang, M. Hou, T. Zhang, B. Li, P. Xue, Y. Kang and Z. Xu, *Chem. Commun.*, 2018, DOI: 10.1039/C8CC02261E.

ROYAL SOCIETY OF CHEMISTRY

rsc.li/chemcomm

ChemComm

View Article Online
DOI: 10.1039/C8CC02261E

COMMUNICATION

Water-soluble Fluorescent Unimolecular Micelles: Ultra-small Size, Tunable Fluorescence Emission from Visible to NIR Region and Enhanced Biocompatibility for In Vitro and In Vivo Bioimaging

Received 00th January 20xx,
Accepted 00th January 20xx

DOI: 10.1039/x0xx00000x

www.rsc.org/

Xiaoqian Ma[a, b], Xiaoxiao Shi[a, b], Shuang Bai[a, b], Jianjian Zhang[c], Meili Hou[a, b], Tian Zhang[a, b], Bao-sheng Li[d], Peng Xue[a, b], Yuejun Kang[a, b]*, Zhigang Xu[a, b]*

Fluorescent unimolecular micelles (FUMs) with multicolor emission acting as fluorescent nanoagents for optical fluorescence imaging are firstly reported. The FUMs show good water-solubility, ultra-small size, enhanced biocompatibility,which endow the FUMs with versatile applications including organelles labeling, multicolor markers and high tumor accumulation, revealing that our design can serve as a rational strategy for the development of UM-based fluorescent nanoagents for bioprocess monitoring.

Fluorescence-based imaging nanoagents (FIN) utilizing fluorophores have been emerging as an effective and noninvasive strategy for diseases diagnosis and monitoring, the guide of surgical interventions and the assessment of treatment outcome.[1] In comparison with magnetic imaging, computed tomography (CT), radioactive imaging and ultrasound imaging, FIN, which only employs a simple but practical light to realize the generation of detection signal without extra concern such as hazardous optical radiation and poor spatial resolution, have attracted tremendous attention for therapeutics.[1c] Although many fluorophores-based organic[2] or inorganic[3] materials have been prepared for optical imaging, their use in clinical practice are still hampered by the following issues: (i) the inherent heavy-metal (e.g., Pb or Cd) toxicity and lengthy biodegradability period;[4] (ii) most organic fluorophores sharing the drawbacks of aggregation-caused quenching (ACQ) effect, poor photostability and small Stokes shifts.[5] Nevertheless, organic fluorophores have been served as a preferential choice for bioimaging because of their non-invasiveness, low-toxicity, high sensitivity and broad detection region.

Polymeric fluorescent nanoagents (PFNs) with well-defined structure, flexible decoration, high biocompatibility and other virtues impelled a class of fluorescent agents for optical imaging.[6] In addition, the ingredients of PFNs are thoroughly organic, and thus heavy-metal toxicity can be avoided spontaneously.[7] To achieve the biocompatibility and water-solubility, the fluorophores are usually linked to a polymeric backbone, including dendrimers,[8a] polyethylene glycol (PEG) [8b] and dendronized polyols,[8c] which can avert the effect of nonspecific binding while dramatically improve their imaging capability. In comparison with small fluorescent molecular agents, fluorescent nanoagents exhibit an ultrasensitive detection at nanomolar-picomolar level.[9] Thus, organic fluorescent nanoagents that integrate water-solubility, nano-size effect and biocompatibility into one system can properly facilitate their biological application in cellular or molecular level, representing an effective strategy.

As a polysaccharide, β-cyclodextrin (β-CD) provides specific chemical structure, natural biocompatibility and biodegradability, which shows huge potential to be used as the multi-arms reactor for the development of star-like copolymers.[10] We previously have synthesized a series of β-CD-based amphipathic star-like polymers through atom transfer radical polymerization (ATRP) by direct polymerization hydrophobic or hydrophilic monomers with the β-CD macroinitiator, producing robust and water-soluble unimolecular micelles (UMs) in aqueous medium.[11] Inspired by this point, the strategy should be expanded to create a kind of UM-based fluorescent nanoagent, providing an expectant application for biolabeling and bioimaging.

To achieve this goal, we herein report a series of fluorescent star-like copolymers (β-CD-P(Dye-*co*-OEGMA) using β-CD as core and different fluorophores as polymeric shell. This rational design can endow the targeted copolymer with high-

[a] *Institute for Clean Energy and Advanced Materials, Faculty of Materials and Energy, Southwest University, Chongqing 400715, P. R. China.*
[b] *Chongqing Engineering Research Centre for Micro-Nano Biomedical Materials and Devices, Chongqing 400715, P.R. China. Email: zgxu@swu.edu.cn; Fax: +86-68253204; Tel: +86-68253792; yjkang@swu.edu.cn; Fax: +86-68253204; Tel: +86-68254056*
[c] *Key Laboratory of Synthetic and Natural Functional Molecule Chemistry of Ministry of Education, College of Chemistry and Materials Science, Northwest University, Xi'an, Shaanxi 710127, P. R. China*
[d] *School of Chemistry and Chemical Engineering, Chongqing University, 174 Shazheng Street, Chongqing 400044, P. R. China*
Electronic Supplementary Information (ESI) available: [The detailed procedures and characterization of star-like copolymers. The supplementary results of cytotoxicity and confocal imaging results]. See DOI: 10.1039/x0xx00000x

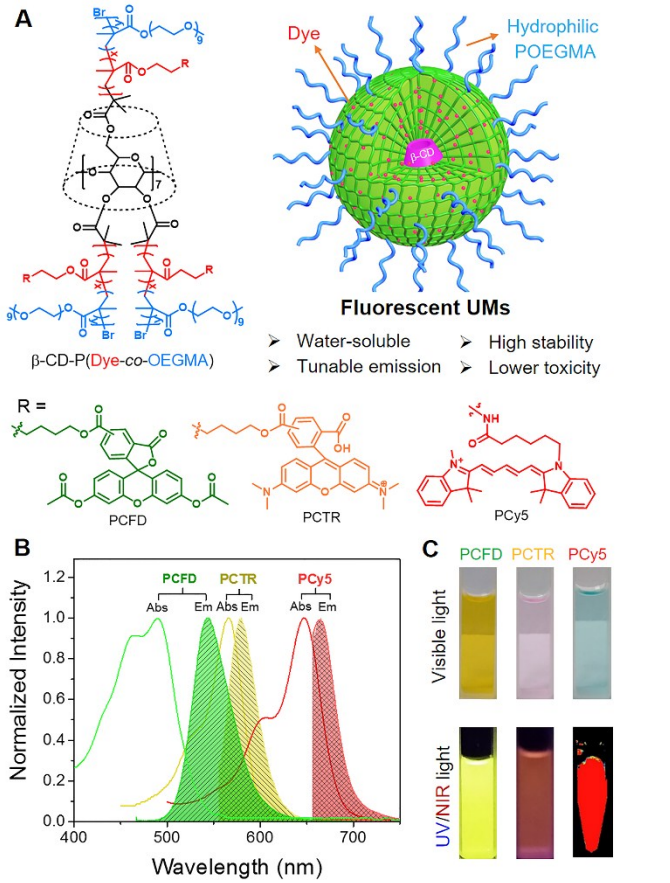

Fig.1 (A) The chemical structure of amphipathic star-polymer copolymer of β-CD-P(Dye-co-OEGMA) (Dyes: CFD, CTR or Cy5), and the schematic illustration of fluorescent unimolecular micelles (FUMs). (B) Normalized absorption and emission spectra of PCFD, PCTR and PCy5 UMs; (C) The digital photographs of PCFD, PCTR or PCy5 UMs in water medium under visible or UV/NIR light, respectively.

density arms, which can reduce the intermolecular aggregation between the dye moiety and the hydrophilic POEGMA chain,[12] protect the fluorescence intensity of dyes and conveniently form monodisperse fluorescent unimolecular micelles (FUMs) in aqueous medium. Specifically, these FUMs with good water-solubility, ultra-small size (~30 nm) and tunable fluorescence emission from visible to NIR region can be used as a powerful imaging tool for bioprocess monitoring. To verify the generality of the FUM design, three commercial dyes （5(6)-carboxyfluorescein diacetate (CFD), 5(6)-carboxy-tetramethylrhodamine (CTR) and cyanine 5-NHS ester (NHS-Cy5)） with different emissive wavelength were selected to construct the polymerized dye monomers. To regulate the water-solubility, a hydrophilic moiety of oligo (ethylene glycol) methyl ether methacrylate (OEGMA) was used to polymerize together with these dye monomers for constructing the polymeric shell of the star-like copolymers through a brief step as described in the ESI†. Finally, three FUMs of PCFD, PCTR and PCy5 UMs, were obtained *via* dialysis method and were used to realize their imaging capacity.

The synthetic route of the PCFD, PCTR and PCy5 copolymers were presented in Fig. S1-3 (ESI†). For these synthesis, two fluorescent monomers, namely, CFD monomer (MCFD) and CTR monomer (MCTR) were firstly synthesized and characterized (ESI†). Next, three kinds of amphiphilic star-like copolymers [denoted as β-CD-P(MCFD-*co*-OEGMA) (PCFD), β-CD-P(MCTR-*co*-OEGMA) (PCTR), β-CD-P(MCy5-*co*-OEGMA) (PCy5)] with the same β-CD core and hydrophilic POEGMA chain, but different types of dye moieties, were synthesized *via* ATRP reaction that enabled the construction of target polymer with mild and facile synthetic steps. More details of experiment were presented in supporting information. The chemical structures of intermediates and target polymers were characterized with nuclear magnetic resonance (NMR) spectrum and mass spectrum (Fig.S4-9, ESI†). Meanwhile, the polymerization process was monitored by gel permeation chromatography (GPC) technology, and the results in Fig.S10 (ESI†) clearly provided an evidence to demonstrate the well-define structures of three targeted copolymers.

The success of structural information described above encourages us to further establish the micellar formation in water medium using the amphipathic feature of targeted copolymers. The FUMs, which were prepared *via* a dialysis method, possessed a typical spherical shape (Fig. S11A, ESI†) and similar average diameters of ~30 nm (Fig. S11B, ESI†) as shown by transmission electron microscopy (TEM) and dynamic light scattering (DLS), respectively. In addition, the decoration of POEGMA chain endow the resulting polymers with good solubility in aqueous medium without concerns of their biocompatibility. It has been observed that nanoparticles < 50 nm in diameter showed an enhanced accumulation and tumor inhibition ability through enhanced permeability and retention (EPR) effect,[13] leading to an improving biomedical effects for FUMs.

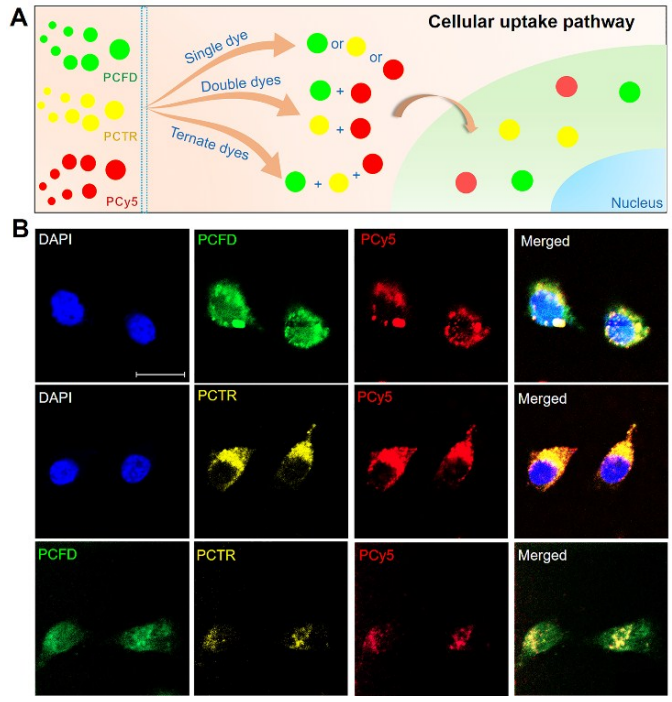

Fig.2 (A) Schematic illustration of the cellular uptake pathway of three FUMs with different mixed patterns. (B) CLSM images of HeLa cells after soaking with PCFD/PCy5, PCTR/PCy5 or PCFD/PCTR/PCy5 for 6 h, respectively. The concentration of FUMs is 20 μg/mL. The fluorescence of CFD, CTR, Cy5 and DAPI were labeled green, yellow, red and blue, respectively. Scale bars: 25μm.

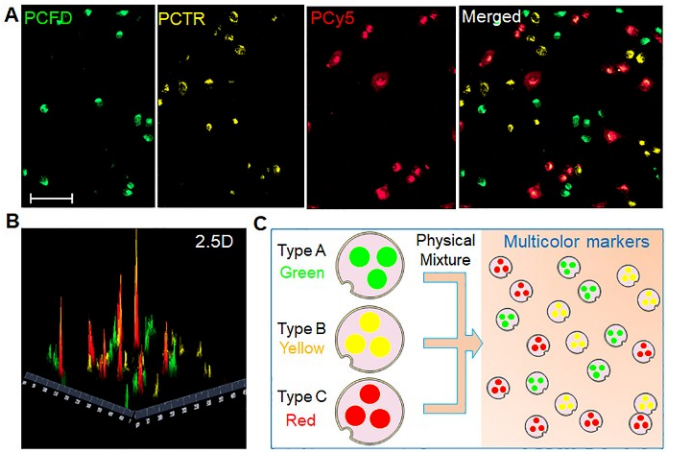

Fig. 3 (A) CLSM images of HeLa cells by physical mixture after incubated with PCFD, PCTR and PCy5 UMs for 6 h. (B) The 2.5-dimensional (2.5 D) image of merged photos. (C) The mechanism representative chart was attached. The fluorescence of CFD, CTR and Cy5 were labeled green, yellow, and red. Scale bars: 50μm

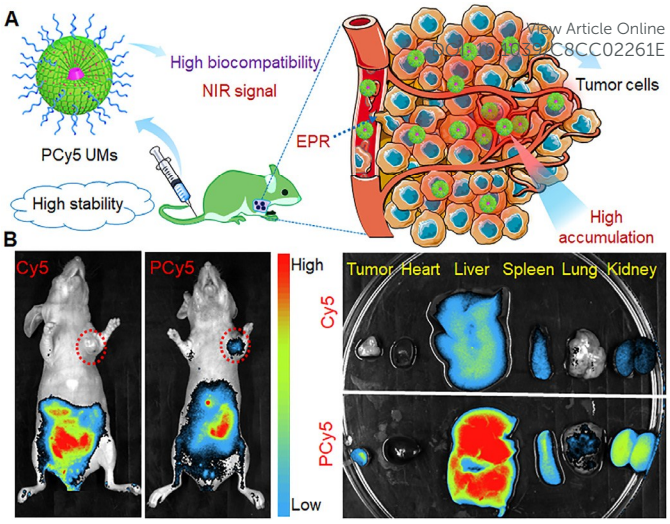

Fig.4 (A) Schematic illustration of the accumulated mechanism of in vivo fluorescent imaging of PCy5 UMs; (B) Whole-body NIR imaging of mice bearing xenograft MCF-7 tumors treated with Cy5 and PCy5 UMs. The tumors were labeled with red dashed circles. (C) Ex vivo fluorescence imaging of the tumors and major organs after a 24 h postinjection.

The photoproperties of PCFD, PCTR and PCy5 were shown in Fig.1 B and Fig.S12 (ESI†). Specifically, the maximum absorption or fluorescence of PCFD, PCTR and PCy5 in water medium were located at 488 or 550 nm, 566 or 580 nm and 647 or 670 nm, respectively, covering a broad detection region from visible to NIR fluorescence. Additionally, the digital photographs of PCFD, PCTR and PCy5 UMs in water medium under the UV light or NIR laser (Fig.1C) showed a green, yellow and red fluorescence, respectively. To test the quantum yield (Φ) of PCFD, PCTR and PCy5 in the micellar form, Rhodamine B in ethanol was selected as the standard,[12b] and the Φ were 100 % (PCFD), 81.46 % (PCTR) and 0.47 % (PCy5) (Table S1, ESI†), respectively. The results revealed that the copolymerization of POEGMA chain could improve the water-solubility and enhanced the fluorescence protection for these FUMs. To investigate the photostability, the fluorescence intensity of FUMs under a continuous irradiation using a LED light (470 nm) were recorded (Fig.S13, ESI†). After 12 h of irradiation, the final fluorescence intensity of FUMs were still maintained above 90 %, suggesting an excellent photostability. These results demonstrated that the POEGMA decoration-based FUMs could not only dramatically protect the photostability of dyes but could effectively suppress the ACQ phenomenon as compared to linear PEG copolymer.[8c]

To verify the potential application of FUMs for bioimaging, the cytotoxicity of three FUMs against HeLa and L929 cells were evaluated using PrestoBlue assay (Fig. S14, ESI†). Upon 72 h incubation, these FUMs with maximum concentration of 50 μg/mL showed slimily negligible cytotoxicity to normal cells, which were benefited from the nature biocompatibility of β-CD core and POEGMA shell. Additionally, the slightly higher toxicity of tumor cells than those of normal cells might be caused by the high accumulation in tumor cells due to the ultra-small size of FUMs.[13a] These data demonstrated the FUMs were promising fluorescent nanoagents as a result of their excellent biocompatibility and high photostability.

The cellular uptake of these FUMs were studied using HeLa cells as the representative tumor cells. The uptake behaviors of HeLa cells stained by single FUMs were firstly studied. As shown in Fig.S15-18 (ESI†), a uniform distribution of each FUM was visualized in the cytoplasm, suggesting a time-dependent intracellular uptake. Additionally, the distribution of FUMs in cells almost overlapped with AF-633, a commercialized fluorescent dye for staining cytoskeleton, showing a targeting ability of FUMs towards cytoskeleton in living cells. The possible reason should be caused by the ultra-small size and the good water-solubility of FUMs, leading to an easy phagocytosis process. The distribution of FUMs in HeLa cells stained by double or ternate FUMs were further investigated (Fig.2 and S19, ESI†). Specifically, a visible fluorescence (PCFD or PCTR) and the NIR fluorescence (PCy5) could be simultaneously imaged by CLSM. Similarly, the performance was also observed in HeLa cells after incubating with a ternate combination of PCFD, PCTR and PCy5. The uptake efficiency determined by flow cytometry further revealed the quickly phagocytized effect of FUMs by HeLa cells (Fig. S20-21, ESI†). The lysosome or mitochondria specific internalized pathway of FUMs were also verified by CLSM using a commercial Lyso Tracker dye (Fig. S22-24, ESI†) and Mito-tracker dye (Fig. S25-26, ESI†). These data not only proved the superior size-dependent distribution of FUMs but also revealed a fact that FUMs can serve as outstanding fluorescent nanoagents for multicolor imaging of organelles without upsetting cross-color phenomenon.

Inspired by these above imaging results, we further explore the potential of these FUMs for multicolor markers in one imaging window, which is highly desirable for multicolor biological assays.[14] For this purpose, HeLa cells was served as the cancer cells model and was firstly treated with PCFD, PCTR or PCy5 FUMs, severally. After 6 h incubation, two or three cellular solutions of FUMs were mixed, and then were co-incubated for additional 6 h for CLSM detection. Interestingly, HeLa cells soaking with ether two (Fig. S27-29, ESI†) or three (Fig.3) mixed FUMs could be clearly observed in one single

window with a multiple wavelength excitation, suggesting an excellent recognition ability depending on the difference of fluorescence emissive FUMs. These results demonstrated that the FUMs showed a predictable potency to understand the nano-bio interactions between nanoagents and cells.

These outstanding *in vitro* results of FUMs including organelles and cells imaging further encourage us to proceed their performance *in vivo*. Firstly, the complete blood assay employing a mouse mode was performed to evaluate the potential toxicology *in vivo* of our FUMs (Fig.S30, ESI†). Specifically, Sprague Dawley (SD) mice were systemically administrated with PBS, PCFD, PCTR and PCy5 UMs through the tail vein, and then a series of blood biochemical parameters were recorded by a haematology analyser.[15] Compared with the control PBS group, the parameters of FUMs group were all in the range of reasonable scope, suggesting an excellent biocompatibility *in vivo* for FUMs.

The fluorescence-imaging potential of FUMs *in vivo* was performed in living mice. After nude mice bearing xenograft MCF-7 tumors were anesthetized, free Cy5 or PCy5 aqueous solutions were systematically injected by the tail intravenous administration (Fig.4). After a 24 h of postinjection, the fluorescence intensity of the mice treated with PCy5 was 2.5-fold higher than free Cy5-treated mice (Fig.S31, ESI†), showing an enhanced accumulation in tumors through EPR-based passive targeting mechanism.[15] Combining with their long-lasting blood circulation driven by the size effect (< 50 nm),[13c] FUMs can be served as a promising nanoagent for tumor localization, and hold huge potential for clinical transformation.

In conclusion, we have provided an effective molecular design strategy to prepare a series of FUMs with outstanding performance for optical fluorescence imaging *in vitro* and *in vivo*. The rational design endow FUMs with ultra-small size, tunable emissive fluorescence and low-toxicity, and can serve as a hopeful imaging nanoagent for organelles labeling and tumor localization. Such a strategy also shows a flexible expansibility for the development of other imaging nanoagents with special functions for other biomedical application such as noninvasive imaging-guided surgery.

This study was financially supported by National Natural Science Foundation of China (51703187 and 31671037), a start-up grant (SWU115058 and SWU115059), Fundamental Research Funds for Central Universities from Southwest University (XDJK2016A010) and the Basic and Frontier Research Project of Chongqing (cstc2016jcyjA0078).

Notes and references

1 (a) G. Hong, A. L. Antaris and H. Dai, *Nat. Biomed. Eng.*, 2017, **1**, 0010; (b) J. V. Frangioni, *Curr. Opin. Chem. Biol.*, 2003, **7**, 626-634; (c) C. Yang, X. Wang, S. Huang and M. Wang, *Adv. Funct. Mater.*, 2017, **7**, 1705226.

2 (a) X. Chen, X. Zhang, L. Xia, H. Wang, Z. Chen and F. Wu, *Nano Lett.*, 2018, **18**, 1159-1167; (b) Z. Xu, D. Wang, M. Guan, X. Liu, Y. Yang, D. Wei, C. Zhao and H. Zhang, *ACS Appl. Mater. Inter.,* 2012, **4**, 3424-3431; (c) M. Liu, H. Zou, C. Li, R. Li and C. Huang, *Chem. Commun.* 2017, **53**, 13047-13050; (d) D. Li, Z. Qiao, Y.Yan, J. Tang, X. He, H. Shi, X.Ye, Y.Lei and K. Wang. *Chem. Commun.,* 2018, **54**, 1089-1092; (e) H. Choi, S. Gibbs, J. Lee, S. Kim, Y. Ashitate, F. Liu, H. Hyun, G. Park, Y. Xie and S. Bae, *Nat. Biotechnol.* 2013, **31**, 148-153. (f) Z. Xu, X. Ma, Y. Gao, M. Hou, P. Xue, C. Li and Y. Kang, *Mater. Chem. Front.* 2017, **1**, 1257-1272.

3 (a) F. de Arquer, A. Armin, P. Meredith and E. Sargent, *Nat. Rev. Mater.,* 2017, **2**, 16100; (b) J. Yu, Y. Rong, C. Kuo, X. Zhou and D. Chiu, *Anal. Chem.,* 2017, **89**, 42-56; (c) O. T. Bruns, T. S. Bischof, D. K. Harris, D. Franke, Y. Shi, L. Riedemann, A. Bartelt, F. B. Jaworski, J. A. Carr, C. J. Rowlands, *Nat. Biomed. Eng.,* 2017, **1**, 0056; (d) H. Ogasawara, M. Grzybowski, R. Hosokawa, Y. Sato, M. Taki and S. Yamaguchi, *Chem. Commun.* 2018, **54**, 299-302. (e) Y. Wang, M. Chen, N. Alifu, S. Li, W. Qin, A. Qin, B. Tang and J. Qian, *ACS Nano,* 2017, **11**, 10452-10461.

4 (a) A. L. Antaris, H. Chen, K. Cheng, Y. Sun, G. Hong, C. Qu, S. Diao, Z. Deng, X. Hu, B. Zhang, X. Zhang, O. K. Yaghi, Z. R. Alamparambil, X. Hong, Z. Cheng and H. Dai, *Nat. Mater.* 2016, **15**, 235-242; (b)D. Avnir, D. Levy and R. Reisfeld, *J. Phys. Chem.*, 1984, **88**, 5956-5959.

5 (a) X. Ma, R. Sun, J. Cheng, J. Liu, F. Gou, H. Xiang and X. Zhou, *J. Chem. Educ.*, 2015, **93**, 345-350; (b) F. Hu, X. Cai, P. Manghnani, K. Kenry, W. Wu and B. Liu, *Chem. Sci.*, 2018, **9**, 2756-2761.

6 (a) C. F. Wu, S. Hansen, Q. Hou, J. Yu, M. Zeigler, Y. Jin, D. Burnham, J. McNeill, J. Olson and D. Chiu, *Angew. Chem. Int. Edit.*, 2011, **50**, 3430-3434; (b) Y. Chan and P. Wu, *Part. Part. Syst. Char.*, 2015, **32**, 11-28.

7 K. Pu, N. Chattopadhyay and J. Rao, *J. Control. Release*, 2016, **240**, 312-322.

8 (a) Y. Bai, H. Xing, G. Vincil, J. Lee, E. Henderson, Y. Lu, N. Gabriel Lemcoff and S. Zimmerman, *Chem. Sci.*, 2014, **5**, 2862-2868;(b) J. Liu, D. Ding, J. Geng and B. Liu, *Polym. Chem.*, 2012, **3**, 1567-1575; (c) Y. Li, Y. Bai, N. Zhang, Y. Liu, G. Vincil, B. Pedretti, J. Cheng and S. Zimmerman, *Chem. Commun.,* 2016, **52**, 3781-3784.

9 (a) X. Qian, X. Peng, D. Ansari,Q. Yin-Goen, G. Chen, D. Shin, L. Yang, A. Young, M. Wang and S. Nie, *Nat. Biotechnol.,* 2008, **26**, 83-90; (b) Y. Wang, K. Zhou, G. Huang, C. Hensley, X. Huang, X. Ma, T. Zhao, B. Sumer, R. DeBerardinis and J. Gao, *Nat. Mater.,* 2014, **13**, 204-212.

10 (a) J. Xu and S. Liu, *J. Polym. Sci. Pol. Chem.,* 2009, **47**, 404-419; (b) Z. Tian, C. Chen and H. R. Allcock, *Macromolecules*, 2013, **46**, 2715-2724; (c) X. Pang, L. Zhao, C. Feng and Z. Lin, *Macromolecules*, 2011, **44**, 7176-7183; (d) Q. Zhang, L. Su, J. Collins, G. Chen, R. Wallis, D. A. Mitchell, D. M. Haddleton and C. R. Becer, *J. Am. Chem. Soc.*, 2014, **136**, 4325-4332.

11 (a) X. Shi, X. Ma, M. Hou, Y. Gao, S. Bai, B Xiao, P. Xue, Y. Kang, Z. Xu and C. Li, *J. Mater. Chem. B*, 2017, **5**, 6847-6859; (b) X. Shi, M. Hou, S. Bai, X. Ma, Y. Gao, B Xiao, P. Xue, Y. Kang, Z. Xu and C. Li, *Mol. Pharmaceut.,* 2017, **14**, 4032-4041; (c) Z. Xu, S. Liu, H. Liu, C. Yang, Y. Kang and M. Wang, *Chem. Commun.,* 2015, **51**, 15768-15771.

12 (a) M. Leclerc and J.-F. Morin. Design and Synthesis of Conjugated Polymers; John Wiley and Sons, 2010; (b) C. Yang, H. Liu, Y. Zhang, Z. Xu, X. Wang, B. Cao and M. Wang, *Biomacromolecules*, 2016, **17**, 1673-1683.

13 (a) H. Cabral, Y. Matsumoto, K. Mizuno, Q. Chen, M. Murakami, M. Kimura, Y. Terada, M. R. Kano, K. Miyazono, M. Uesaka, N. Nishiyama and K. Kataoka, *Nat. Nanotech.* 2011, **6**, 815-823; (b) H.J. Li, J.Z. Du, X.J. Du, C.F. Xu, C.Y. Sun, H.X. Wang, Z.T. Cao, X. Z. Yang, Y.H. Zhu, S.M. Nie and J. Wang, *Proc. Natl. Acad. Sci. U. S. A.,* 2016, **15**, 4164-4169; (c) E. Blanco, H. Shen and M. Ferrari, *Nat. Biotechnol.* 2015, **33**, 941-951.

14 A. Tong, Z. Li, G. S. Jones, J. J. Russo and J. Ju, *Nat. Biotechnol.,* 2001, **19,** 756-759.

15 J. Qi, Y. Fang, R. Kwork, X. Zhang, X. Hu, J. Lam, D. Ding and B. Tang, *ACS Nano*, 2017, **11**, 7177-7188.

